

# Data-driven Intra-Autonomous Systems Graph Generator

Caio V. Dadauto, Nelson L. S. da Fonseca, and Ricardo da S. Torres

**Abstract**—This paper introduces a novel deep-learning based generator of synthetic graphs that represent intra-Autonomous System (AS) in the Internet, named Deep-generative graphs for the Internet (DGGI). It also presents a novel massive dataset of real intra-AS graphs extracted from the project Internet Topology Data Kit (ITDK), called Internet Graphs (IGraphs). To create IGraphs, the Filtered Recurrent Multi-level (FRM) algorithm for community extraction was developed. It is shown that DGGI creates synthetic graphs which accurately reproduce the properties of centrality, clustering, assortativity, and node degree. The DGGI generator overperforms existing Internet topology generators. On average, DGGI improves the Maximum Mean Discrepancy (MMD) metric 84.4%, 95.1%, 97.9%, and 94.7% for assortativity, betweenness, clustering, and node degree, respectively.

**Index Terms**—Machine learning, Graphs and networks, Internet Topology, Topology Generator

## I. INTRODUCTION

GENERATING graphs that represent realistic network topologies is crucial for modeling, as well as for assessing novel Internet solutions [1], [2], such as routing strategies, traffic management, and fault detection [3]–[5]. Moreover, large datasets of realistic network topologies are essential for training data-driven models based on graphs [3]–[5]. However, topology generators that capture multiple features of the Internet topology are still unavailable [5].

Node connections in the Internet topology graphs are largely modeled by heavily tailed distribution [6]. The Barábsi-Abert (BA) [7] algorithm is the most popular one for generating scale-free networks (*i.e.*, networks for which power-law distribution can model the node relations), and it has served as the basis for several topology generators [8]–[11].

Most of Internet topology graph generators are structure-based and focus on inter-AS topologies [12]–[17]. Moreover, empirical observations are typically used to model the structure of the Internet as a hierarchical composition of graphs. This hierarchy is based on various assumptions, such as scale-free, uniform growth, and function fitting for node degree distribution. However, these assumptions only partially capture the characteristics of subgraphs in the Internet topology, since they essentially rely on a network growth pattern which is ultimately based on a power-law distribution. Structure-based generators have been designed to synthesize graphs

of hundreds of thousands of nodes, *and do not accurately reproduce the properties of AS graphs.*

Although scale-free networks can accurately model the node-degree distribution of graphs, generators based on power-law assumptions do not capture other relevant graph properties [18], such as centrality and clustering [19]. While centrality encodes information related to the occurrence of hubs, clustering involves the density of a group of nodes. Both characteristics are relevant for various analyses, such as that of tolerance to security in Internet topologies, which is influenced by the number of hubs and their density [20].

On the other hand, data-driven solutions for various different Internet applications have relied on trivial topologies and are typically based on only a few samples of real networks, or on synthetic ones generated by BA-based models [3]–[5]. However, the use of unrealistic topologies may produce misleading assessments of the effectiveness of the performance of new solutions [20]–[22].

In this paper, we propose a data-driven graph generator based on deep learning, named Deep-generative graphs for the Internet (DGGI). It accurately reproduces the of centrality, clustering, assortativity, and node degree metrics of Internet graphs. DGGI allows the customization of synthetic graphs, and it can also generate an arbitrary number of synthetic parameterized graphs. To the best of our knowledge, this is the first paper to propose an intra-AS graph generator based on deep learning.

This paper also introduces a novel dataset of intra-AS subgraph extracted from sets of large intra-AS graphs (millions of nodes), named IGraphs. It was collected from the project ITDK conducted by the Center for Applied Internet Data Analysis (CAIDA) [23]. Such extraction employs the Filtered Recurrent Multi-level (FRM) algorithm, which was designed to capture the node agglutination patterns found in the Internet and ensure that the sizes of the subgraphs will be in a predefined range. IGraphs is especially useful for training DGGI.

The main contributions of this paper are:

- the introduction of a novel generator (DGGI) based on deep learning for the generation of intra-AS graphs that encodes not only the node degree distribution of training data but also their centrality, clustering, and assortativity;
- the introduction of an algorithm for the extraction of subgraphs from large networks, that captures the characteristics of large graphs;
- the presentation of a new dataset composed of real intra-AS graphs (IGraphs) extracted from the project ITDK.

C. V. Dadauto and N. L. S. da Fonseca are with the Institute of Computing, UNICAMP – University of Campinas, Brazil. e-mail: {caio.dadauto, nfonseca}@ic.unicamp.br

R. da S. Torres is with the Department of ICT and Natural Sciences, NTNU – Norwegian University of Science and Technologies, Ålesund, Norway. e-mail: ricardo.torres@ntnu.no and Wageningen Data Competence Center, Wageningen, The Netherlands. email: ricardo.dasilvatorres@wur.nl

Compared with existing generators for the Internet, DGGI improves the Maximum Mean Discrepancy (MMD) similarity index [24], [25], on average, 84.4%, 95.1%, 97.9%, and 94.7% for assortativity, betweenness, clustering, and node degree, respectively. In the worst case, DGGI improves 13.1% for assortativity, and, in the best case 99.8% for clustering.

This paper is organized as follows: Section II presents related work focused on generators for Internet topology graphs; Section III shows the graph metrics used for the assessment of the proposed solution; Section IV introduces the DGGI; Section V introduces the IGraphs dataset; Section VI describes the evaluation procedures adopted to validate the DGGI generator and discusses the obtained results. Section VII points out some conclusions and directions for future work.

## II. RELATED WORK

This section describes existing work related to graph generation to represent Internet-like topologies. Table I summarizes the characteristics of the referenced work and shows how the DGGI differs from other generators. The models are classified based on the applicability of their generated graphs for deep learning training. Generators classified as “Suitable for DL” (vide Table I) can synthesize realistic graphs for an arbitrary number of nodes, *i.e.*, they are not restricted to the generation of large graphs with hundreds of thousands of nodes.

Most generators employ algorithms based on scale-free networks and power-law node degree distribution [8]–[17]. The models in [12]–[15] aim at generating graphs as a composition of subgraphs (structures), *e.g.*, AS nodes, core, and periphery.

The BA algorithm [7] is based on the preferential attachment property, *i.e.*, nodes with the highest node degree values tend to have new links attached to them. The Boston University Representative Internet Topology Generator (BRITE) [8] implements the BA algorithm for generating Internet graphs for both inter-AS and intra-AS topologies.

A set of generators based on the BA algorithm has been proposed to introduce new strategies for the preferential attachment paradigm to enhance the ability to generate more realistic graphs. The Extended Barábasi-Abert (EBA) algorithm randomly modifies links beyond the preferential attachment [10]. The Bianco-Barábasi (BB) algorithm introduces a set of parameters (fitness weights) to specialize the preferential attachment mechanism [10]. In contrast, the Dual Barábasi-Abert (DBA) algorithm changes the number of links to be attached to new nodes in a random way [9]. The BB algorithm can reproduce the empirical power-law decays for AS graphs [26], although, the generated graphs are general-purpose ones, *i.e.*, they are not specific to Internet graphs.

Generators based on structure decomposition have been proposed to mitigate the limitations of BA-based generators in reproducing Internet graph properties. The Simulates Internet graphs using the Core Periphery Structure (SICPS) [12] model partitions the Internet graphs into 16 structures that represent different statistical assumptions, including the power-law distribution. The SubNetwork Generator (SubNetG) [13] represents sub-networks and routers as a bipartite graph on the basis of their power-law distribution. The Structure-Based Internet

Topology generator (S-BITE) [14] and Internet AS Graph (IAG) [16] generators use similar approaches to decompose the Internet into core and periphery, each with a different power-law distribution. The Jellyfish [15] generator captures the core (referred to as the ring) of the Internet topology., which relies on the assumption of a power-law distribution.

However, both structure-based generators and the BA-based generators rely on the assumption of power-law distribution, which restricts the generalization of node connectivity, since the decay parameter of a power-law distribution is not sufficient to represent the topology diversity in the Internet [6].

An alternative proposal consists of employing various different structuring procedures. The Orbis generator [17], for example, creates Internet graphs by adopting the  $dK$ -distributions as a criterion to maintain the correlation node degree of subgraphs of size  $d$ . Orbis uses  $1K$  and  $2K$  distributions, which refer to the node degree and the joint node degree distributions, respectively. Despite the fact that the  $dK$ -distributions attempt to unify a wide range of graph metrics [17], they focus only on the node degree, which can lead to a poor representation of other graph properties, such as clique formation and node centrality.

All of these aforementioned generators, however, have been validated only through the inspection of the first-order moments of the selected metrics (as indicated in Table I). In contrast, DGGI generators do not depend on power-law assumption, and the modeling is not focused only on the node degree. Moreover, our evaluation is not restricted to the first-order moments of graph properties; we explore higher-order moments using the MMD metric to quantify the similarity between distributions of graphs.

## III. GRAPH METRICS

Four graph metrics are utilized in the analysis of the properties of the generated graphs: node degree, coefficients of clustering, betweenness, and assortativity [27].

Let  $G$  be an undirected graph with  $N$  nodes, and  $A \in \{0, 1\}^N$  be the adjacent matrix of the graph  $G$ . The node degree is the number of connections of a node, *i.e.*, the node degree of the  $i$ -th node is

$$\kappa_i = \sum_j^N A[i, j] \in \mathbb{N}, \quad (1)$$

in which  $A[i, j]$  is the element on the  $i$ -th row and  $j$ -th column of the adjacent matrix.

The clustering metric indicates the tendency of a node to cluster with its neighbors, *i.e.*, the occurrence of density-connected regions in the graph. The clustering coefficient for the  $i$ -th node is defined as

$$C_i = 2 \frac{l_i}{\kappa_i(\kappa_i - 1)} \in [0, 1] \quad (2)$$

in which  $l_i$  is the number of edges between the neighbors of node  $i$ . Moreover, the global clustering coefficient can also be defined as

$$C = \frac{N_\Delta}{N_3} \in [0, 1] \quad (3)$$

TABLE I  
OVERVIEW OF RELATED WORK.

Reference	Technique	Requirements	View	Suitable for DL	Validation
SICPS [12]	Multi-Structure Decomposition	Number of Nodes and Structure Statistical Properties	Inter-AS	No	First-Order Moments of Node Degree, Assortativity, and Clustering
SubNetG [13]	Scale-free and Hierarchical Decomposition	Number of Nodes and Component Power Law Coefficients	Intra-AS	No	First-Order Moments of Node Degree and Clique Sizes
S-BITE [14]	Scale-Free and Core-Periphery Decomposition	Number of Nodes and Core-Periphery Statistical Properties	Inter-AS	No	First-Order Moments of Node Degree, Clustering, Betweenness, Closeness, and Clique Size
Jellyfish [15]	Scale-Free and Ring Decomposition	Number of Nodes and Ring Power Law Coefficients	Inter-AS	No	First-Order Moments of Node Degree
IAG [16]	Scale-free and Hierarchical Decomposition	Number of Nodes	Inter-AS	No	First-Order Moments of Node Degree
Orbis [17]	$dK$ -Series Preservation	Number of Nodes and $dK$ -Series	Both	No	First-Order Moments of Node Degree and Betweenness
BRITE [8]	Barábasi-Abert	Number of Nodes and Preferential Attachment Coefficients	Both	Yes	First-Order Moments of Node Degree
DBA [9]	Dual Barábasi-Abert	Number of Nodes and Preferential Attachment Coefficients	–	Yes	–
BB [10]	Bianco-Barábasi	Number of Nodes and Preferential Attachment Coefficients	–	Yes	First-Order Moments of Node Degree
EBA [11]	Extended Barábasi-Abert	Number of Nodes and Preferential Attachment Coefficients	–	Yes	First-Order Moments of Node Degree
DGGI-based (our)	Deep Learning	Number of Nodes and DL Weights	–	Yes	Multi-Order Moments of Node Degree, Clustering, Betweenness, and Assortativity

– : No applicable

in which  $N_\Delta$  is the number of triangles in the graph, and  $N_3$  is the number of connected triads of nodes.

The betweenness metric indicates the importance of a node in relation to the number of shortest paths that pass through it. Since hubs usually have a central role in graphs, nodes in a hub tend to present a larger betweenness coefficient. Formally, the betweenness for the  $i$ -th node can be defined as

$$\mathcal{B}_i = \sum_{\substack{p \neq i \neq q \in \{1, \dots, N\} \\ p \neq q}} \frac{\sigma_i(p, q)}{\sigma(p, q)} \in [0, 1] \quad (4)$$

in which  $\sigma_i(p, q)$  is the number of shortest paths between the  $p$ -th and  $q$ -th nodes that pass through the  $i$ -th node, and  $\sigma(p, q)$  is the total number of shortest paths between  $p$  and  $q$ .

The assortativity metric indicates the preferential connectivity of nodes of different node degrees, *i.e.*, whether or not the network growth follows the preferential attachment pattern.

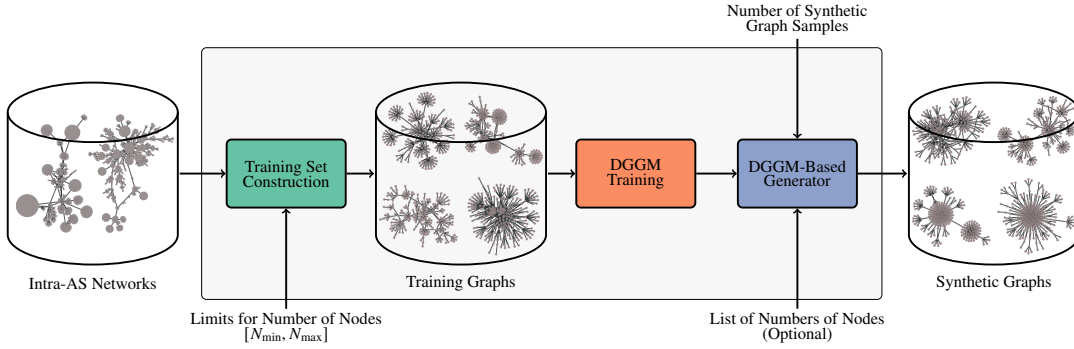


Fig. 1. Procedures used to instantiate DGGI: the training set construction, the DGGM training, and the synthetic graph generation based on DGGM.

Assortativity is a scalar measure that is defined as

$$r = \frac{\sum_k e_{kk}}{\sum_k \alpha_k \beta_k} \in [-1, 1], \quad (5)$$

where  $k$  is the node degree of graph  $G$ ,  $\alpha_k = \sum_{k'} e_{kk'}$ ,  $\beta_k = \sum_{k'} e_{k'k}$ , and  $e_{kk'}$  is the number of edges of nodes with degree  $k$  and nodes with degree  $k'$ .

#### IV. DEEP-GENERATIVE GRAPHS FOR THE INTERNET (DGGI) MODEL

Figure 1 illustrates the three procedures used to instantiate the DGGI generator: the construction of the training set based on the application of the FRM algorithm, the training of the deep-generative graph model; and the generation of synthetic graphs.

For the construction of the training set, the input is a set of samples from large intra-AS networks, with lower and upper bounds reflecting the number of nodes. The final training dataset contains only graphs with a given number of nodes in the defined range.

The Deep Graph Generative Model (DGGM) is then trained using the training graphs created during this first procedure. The final procedure is then responsible for using the trained model to synthesize intra-AS graphs based on two parameters: an optional list that defines the number of nodes and the number of graph samples. When not specified, the range defined is that of the construction of the training set.

The implementation of each procedure is outlined next.

##### A. Training Set Construction

To extract subgraphs with a size bounded by a pre-defined limit, we introduce the FRM algorithm, which recursively employs a multi-level algorithm [28], followed by the use of a filter based on betweenness centrality to avoid a single star topology. The multi-level algorithm aims at defining the communities which maximize the node's local contribution to the overall modularity score. This score measures the ratio between the density of intra and inter-community links.

The recursive application of the multi-level algorithm may lead to graphs with a single hub (graph with a star topology), due to the high disparity between intra and inter-hub links observed in subgraphs with a large number of hubs and

---

#### Algorithm 1 Filtered Recurrent Multi-level (FRM)

---

**Require:** A graph  $G$ , the minimum ( $N_{\min}$ ) and the maximum ( $N_{\max}$ ) of the number of nodes.

```

1: to_process = [G]
2: training_set = []
3: while |to_process| > 0 do
4:   G = to_process.pop()
5:   N = number_of_nodes(G)
6:   if N > N_max then
7:     clusters = multilevel(G)
8:     if |clusters| > 1 then
9:       to_process = concat(to_process, clusters)
10:    end if
11:  else
12:    if N > N_min and |[B1, ..., BN] > 0| > 1 then
13:      training_set = concat(training_set, clusters)
14:    end if
15:  end if
16: end while
17: return training_set

```

---

low clustering coefficients. In order to avoid the redundant occurrence of hubs in the training dataset, all subgraphs defined by a single hub are discarded using the aforementioned filter.

Algorithm 1 presents the FRM algorithm used for the construction of the training set. The lists defined in the first two lines control the process of subgraph extraction. The list *to\_process* contains the graphs that must be split into smaller subgraphs, while the list *training\_set* contains the subgraphs that actually define the training set. The block defined between Lines 5 and 9 employs the multilevel algorithm that splits those graphs with a number of nodes greater than  $N_{\max}$  into subgraphs. The condition in Line 6 ensures that the subgraphs are pushed to *to\_process* only if the multilevel algorithm has been capable of splitting the graph, otherwise it is ignored. The condition in Line 12 ensures that the training set will only be composed of graphs with a number of nodes greater than or equal to the parameter  $N_{\min}$ , and with a topology different from a star, *i.e.*, a topology that has more than one node with a betweenness coefficient greater than zero. The complexity of the algorithm FRM is bounded by  $O(N)$

---

**Algorithm 2** GraphRNN

---

**Require:** The maximum number of nodes  $\max_N$ , the latent dimension  $L$ , the transient dimension  $M$ , two GRU layers,  $f : (\mathbb{R}^M, \mathbb{R}^L) \mapsto \mathbb{R}^L$  and  $g : (\mathbb{R}, \mathbb{R}^L) \mapsto \mathbb{R}$ , the initial graph state  $h_g$ , and the start and end tokens,  $SOS \in \mathbb{R}^M$  and  $EOS \in \mathbb{R}^M$ .

```

1:  $s_1 = SOS$  and  $i = 1$ 
2: for each  $i \in \{1, \dots, \max_N\}$  do
3:    $h_g = f(s_i, h_g)$ 
4:    $s_{i+1} = s_i$ 
5:   for each  $j \in \{1, \dots, \min(i - 1, M)\}$  do
6:      $h_o = g(s_{i+1}[j], h_g)$ 
7:      $s_{i+1}[j] = h_o$ 
8:   end for
9: end for
10: return  $\{s_1, \dots, s_{N_{\max}}\}$ 

```

---

and  $O(2^h N)$  for the best and the worst cases, those for  $\log_2\left(\frac{N}{N_{\min}}\right) \geq h \geq \log_2\left(\frac{N}{N_{\max}}\right)$  with  $N$  being the number of nodes of the input graph  $G$ .

### B. Deep Graph Generative Model Training

DGGI uses the recently proposed GraphRNN [25] as the deep-generative graph model. This model is a general-purpose data-driven generator of synthetic graphs based on deep learning. The architecture of the GraphRNN comprises two different hierarchical Gate Recurrent Unit (GRU) [29], one to embed the graph state and the other to predict the new connections for each node. GRU is a variation of recurrent neural networks specialized in embedding relations established by long-ordered sequences of tensors into a state, a vector with a pre-defined dimension (so-called latent dimension). GraphRNN maps the graph generation into a sequential procedure based on edges added to each node. In order to make this feasible, GraphRNN establishes a node order for processing all graphs during the training.

There is no unique node order to represent a graph using a sequence of nodes. In fact, the number of possible representations of such a graph based on sequences is  $n!$  with  $n$  being the number of nodes [25]. The pre-defined node order is used by GraphRNN to reduce the number of possible node permutations, thus improving learning efficiency [25]. GraphRNN uses the node order established by the Breadth First Search (BFS) algorithm since different node permutations can be mapped onto a unique node order [25].

Formally, let  $G$  be a graph with  $N$  nodes defined by a given order. A sequence to represent the graph  $G$  is described as  $s = (s_1, \dots, s_N)$ , with  $s_i \in \{0, 1\}^{i-1}$  being the vector representing all connection between the node  $i$  and the remaining  $i - 1$  nodes. Assuming the BFS order for the nodes, the dimension of vector  $s_i \forall i$  can be bounded by a fixed number  $M$  [25], the transient dimension. Therefore, a vector  $s_i \forall i \in \{2, \dots, N\}$  can be redefined as

$$s_i = [A[\max(i, i - M), i], \dots, A[i - 1, i]], \quad (6)$$

where  $A[i, j]$  is the element of the  $i$ -th row and  $j$ -th column of the adjacency matrix of the graph  $G$ .

Algorithm 2 outlines how GraphRNN synthesizes a graph. The loop in Line 2 is responsible for determining all the connections for each new node. These connections are defined for all  $\max_N$  nodes (as defined in Section IV-A). In Line 3, the graph state ( $h_g$ ) is determined by the GRU  $f$  using the connections of  $i$ -th node and the previous graph state. The loop in Line 5 determines the  $\min(i - 1, M)$  connections of the  $(i + 1)$ -th node, in which  $i$  nodes have already been added to the graph. Finally, each  $j$  connection is determined by the second GRU  $g$  using the current graph state and the  $j$ -th connection of the  $i$ -th node. The complexity of Algorithm 2 is  $O(\min(i - 1, M)N_{\max}C_g + N_{\max})$ , where  $C_g$  and  $C_f$  are the respective complexities for GRU layers  $g$  and  $f$ .

### C. Synthetic Graph Generation

The final procedure is responsible for synthesizing intra-AS graphs. It utilizes the trained GraphRNN model. Two parameters are required to generate graphs: the number of synthetic graphs, and, optionally, a list of the number of nodes.

Given a trained GraphRNN, synthetic graphs are created using the output of Algorithm 2. In order to define a graph, the vectors  $\{s_1, \dots, s_{N_{\max}}\}$  provided by the trained GraphRNN is transformed into an adjacency matrix  $A$ . This transformation requires the mapping of the vector values to be 0 or 1 since  $s_i \in [0, 1]^M \forall i$ . A threshold  $\tau$  is used to implement the mapping. The algorithm assigns 1 if the value is larger than  $\tau$  and 0 otherwise.

The use of a fixed value of  $\tau$  will produce the same set of graphs for all runs of Algorithm 2 as a consequence of the fixed weights of GraphRNN. To avoid this, the threshold  $\tau$  can be sampled from a uniform distribution  $\mathcal{U}(]0, 1[)$  for all the different runs of Algorithm 2.

Given the statistical nature of both deep learning models and the threshold  $\tau$ , the adjacency matrix resulting from the former process does not necessarily represent a connected graph. The connected subgraphs provided by the adjacency matrix provide the synthetic graph.

Algorithm 3 outlines how the generator is defined using a pre-trained GraphRNN. In Lines 6 to 8 the threshold, an empty adjacent matrix, and the node states are defined, respectively. The loop in Line 10 maps each vector state  $s_j$  to the proper column of the adjacency matrix using the threshold  $\tau$  and the transient dimension  $M$  (defined in Section IV-B). The loop in Line 16 extracts all connected subgraphs from the adjacency matrix. Only the subgraphs with a number of nodes included in the list  $L$  are considered. The algorithm stops when the number of synthetic graphs is greater than or equal to  $T$ . The generation of each graph has complexity bounded by  $O(C_{\mathcal{F}} + N_{\max}^2)$  and  $O(C_{\mathcal{F}} + N_{\max}^2 + M^2 - N_{\max}M)$ , where  $C_{\mathcal{F}}$  is the complexity of GraphRNN.

## V. THE INTERNET GRAPHS (IGRAPHS) DATASET

This section describes the construction of the proposed intra-AS graph dataset, IGraphs. It also discusses the properties of the graphs produced.

**Algorithm 3** Graph Generator

**Require:** A trained GraphRNN  $\mathcal{F}$ , the number of synthetic graphs  $T$ , and, optionally, the list of numbers of nodes  $L$ , the minimum ( $N_{\min}$ ) and the maximum ( $N_{\max}$ ) of the number of nodes, and the transient dimension  $M$ .

```

1: graphs = []
2: if  $L = \emptyset$  then
3:    $L = \{N_{\min}, \dots, N_{\max}\}$ 
4: end if
5: while  $|graphs| < T$  do
6:    $\tau \sim \mathcal{U}(0, 1]$ 
7:    $A_k = \{0\}^{N_{\max} \times N_{\max}}$ 
8:    $\{s_1, \dots, s_{N_{\max}}\} = \mathcal{F}()$ 
9:   for each  $s_j \in \{s_1, \dots, s_{N_{\max}}\}$  do
10:    for each  $i \in \{\max\{1, j - M\}, j - 1\}$  do
11:     if  $s_j[i] \geq \tau$  then
12:       $A_k[i, j] = 1$ 
13:     end if
14:    end for
15:   end for
16:   for each  $G = \text{connected\_subgraphs}(A_k)$  do
17:    if  $\text{number\_of\_nodes}(G) \in L$  then
18:      $\text{graphs.push}(G)$ 
19:    end if
20:   end for
21: end while
22: return  $graphs$ 
    
```

### A. Graph Construction

The construction of IGraphs follows the procedures described in Section IV-A. The ITDK repository is used for the extraction of graphs to compose IGraphs. ITDK is a CAIDA project that consists of the router connectivity of a cross-section of the Internet. ITDK stores the historical router-level topologies providing the IPv4/v6 traces, the router-to-AS assignments, the router geographic location, and the DNS for all observed IP addresses.

The present procedure uses the IPv4 traces, the geographic locations, and AS assignments. All this information is structured in three different text files. The Internet cross-section provided by ITDK, with more than 90 million nodes, divided into AS subgraphs using the router-to-AS tables and the IPv4 links. The links are pre-processed to extract the edges since more than two nodes can share the same link, *i.e.*, one link can have multiple edges. Then, all edges with the predecessor and the successor within the same AS are labeled as intra-AS edges. This procedure relies on the information provided by the router-to-AS table.

The topologies are simplified to emphasize the router relations, multi-edges (edges with the same pair of predecessor and successor) and self-edges (edges with the predecessor equal to the successor) are discarded. Once the intra-AS edges are defined, the graphs are created.

The number of nodes of graphs in IGraphs ranges from 12 to 250. These limits have been defined based on the number of nodes of graphs often used to evaluate recently

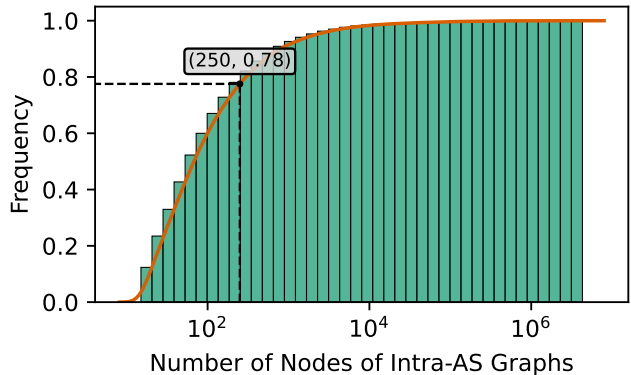


Fig. 2. Cumulative distribution of the numbers of nodes of intra-AS graphs.

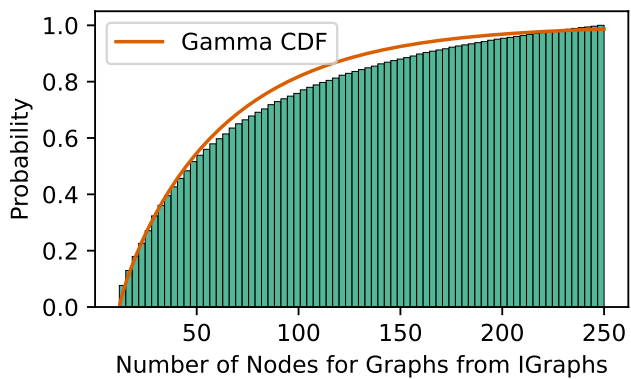


Fig. 3. The cumulative distribution of the numbers of nodes of IGraphs. The orange curve represents the CDF of gamma with parameters fitted to the presented cumulative distribution.

proposed graph-based data-driven models in communication networks [3]–[5], [13]. Nevertheless, the procedure described here can be used for other ranges.

Figure 2 shows the distribution of the number of nodes of an AS-graph, in which 22% of the ASs have at least 250 routers, a number that is out of the range of interest. We also use the remaining set of graphs (those outside the specified range) can also be used, but after the application of the procedures described in Section IV-A to extract the subgraphs that are indeed within the range of interest. The final dataset has 90,326 graphs, each with 12 to 250 nodes. The distribution of the number of nodes is presented in Figure 3.

The dataset also includes features associated with nodes and edges. The geographic locations of routers are used as node features, while the IP addresses of the links are used as the edge features. Although these features are not actually used by DGGI. They can be relevant for training data-driven approaches for other applications.

### B. Analysis of Dataset Properties

This section presents certain properties associated with the created graph dataset. These properties are also compared to

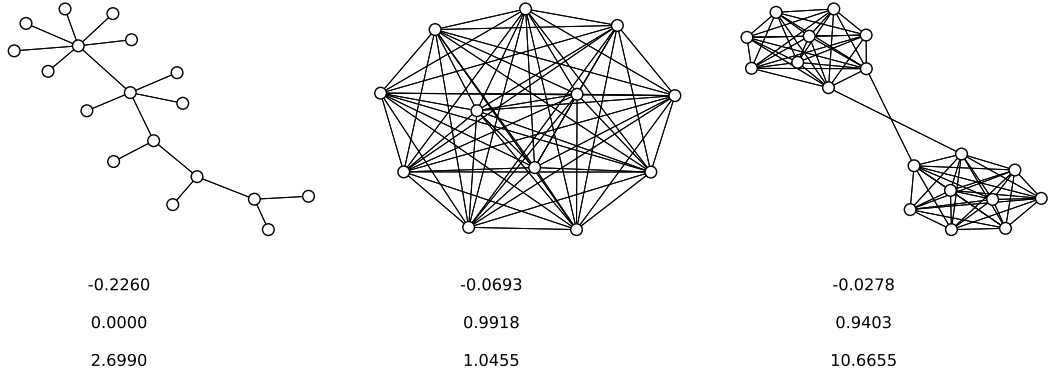


Fig. 4. Examples of graph samples from IGraphs presenting different graph metrics, evaluated in terms of their betweenness ratio, assortativity, and global clustering. The graph on the left does not contain triangles. This leads to a clustering coefficient equal to zero and a low assortativity score. The graph in the middle is a densely connected graph. In this case, the clustering coefficient is high, while the assortativity score is low. The graph on the right contains two hubs. In this case, the betweenness ratio score is high.

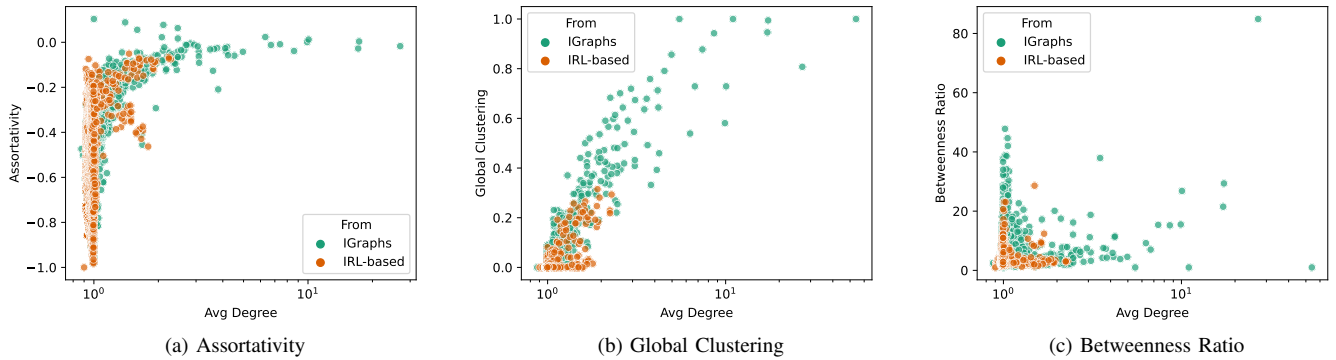


Fig. 5. The scattering of graph properties against the average node degree for IGraphs and the IRL-based datasets. Figures (a) and (b) present the scattering of global assortativity and clustering, respectively; (c), shows the scattering of the ratio between the maximum and the average of betweenness coefficients.

those of a constructed dataset with a dataset constructed based on the Internet Research Lab (IRL) repository<sup>1</sup> [30].

1) *Baseline Dataset*: The IRL repository provides a large cross-section of inter-AS connections. It was selected because most baseline generators are based on this repository [12]–[14], [17].

The procedures described in Section IV-A were also used to extract the subgraphs from the IRL repository. This led to a dataset (1700 graphs) smaller than our dataset, which was expected since the inter-AS level presents fewer nodes. To compare the properties of the two datasets, 1700 graphs from our dataset were randomly selected.

2) *Comparison Metrics*: The analyses presented are based on three graph metrics; the coefficients for assortativity, clustering, and betweenness. For the latter, the ratio between the maximum and average betweenness coefficients. This ratio encodes the number of hop occurrences in each graph [31]. Figure 4 illustrates the computed values associated with the three metrics for three graph samples collected from IGraphs.

3) *Analyses*: Figure 5 shows the scattering of the used graph metrics in relation to the average node degree as com-

puted by the approach adopted in [31]. The global clustering and the assortativity scores were computed as defined in Equations (3) and (5). For the betweenness ratio, the maximum and average values were computed according to Equation (4).

Fig. 5a shows that the graphs from IGraphs with a larger average node degree tend to present null assortativity, and graphs with nodes with a large node degree do not follow the precepts of preferential attachment, in contrast to graphs having small node degrees. In this case, the assortativity is negative indicating an inverse preferential attachment prone. The IRL-based dataset presents a similar behavior. On the other hand, the graphs extracted from the IRL dataset tend to have a small average node degree, which is expected as the inter-AS networks often have fewer links than intra-AS networks.

Figure 5b shows the occurrences of density subgraphs networks in IGraphs in relation to the IRL-based dataset. For graphs with a low average node degree, there is a trend to a monotonic increase in global clustering for both datasets, a trend that is not clearly verified for graphs with a high average node degree. These graphs present a greater dispersion, which indicates that the nodes are not necessarily prone to triangle formation when the node degree increases.

<sup>1</sup><http://konect.cc/networks/topology/> (As of July 2022).



Fig. 5c suggests that hubs are more frequent in IGraphs than those based on the IRL repository. Moreover, a low average node degree leads to a greater probability of hub occurrences. At the same time, the increase in average node degree does not imply a large occurrence of hubs, *i.e.*, the centrality tends to be homogeneous among all the nodes.

The difference between graph properties can be attributed to the difference in the scope of the two datasets. IGraphs comprises intra-AS graphs, while IRL dataset contains inter-AS graphs. Nevertheless, the IGraphs leverages novel possibilities for the analysis of solutions in communication networks.

The 90,326 graph samples from IGraphs allow training data-driven models based on real Internet topologies, instead of augmentation procedures and the use of a few graphs extracted from the Topology Zoo [31] dataset. Training using IGraphs can also improve the capability of generalization, preventing the occurrence of over-fitting, since IGraphs presents large variability in topologies.

Typically, the evaluations of network mechanisms are based either on simulations or emulations running over simple topologies (*e.g.*, grids, stars) or on a few samples from real topologies (*e.g.*, NSF, Geant2, and Germany50) [3]–[5]. On the other hand, the introduction of IGraphs opens opportunities for performing more robust evaluations based on the diversity of real-world topologies.

## VI. EVALUATION OF DGGI

This section describes the procedure followed to assess the effectiveness of the DGGI, instantiated as described in Section IV. The assessment consists of quantifying to the extent generated synthetic topologies differ from real-world intra-AS graphs.

Section VI-A introduces the Maximum Mean Discrepancy (MMD) metric, used to estimate whether two samples are modeled from the same distribution [24]. Section VI-B describes the training procedures, while Section VI-C describes the baseline generators considered in our study. Finally, the results are presented and discussed in Section VI-D.

### A. Maximum Mean Discrepancy (MMD)

Let  $P$  and  $Q$  be two distributions defined in a metric space  $X$ ,  $\mathcal{H}$  be a reproducing kernel Hilbert space (RKHS) with a kernel  $\kappa$ , and  $\phi$  be a function that maps  $X$  to  $\mathcal{H}$ . MMD is defined as

$$\text{MMD}(P, Q) := \left\| \mathbb{E}_{x \sim P} \phi(x), \mathbb{E}_{y \sim Q} \phi(y) \right\| \quad (7)$$

$$= \mathbb{E}_{\substack{x \sim P \\ x' \sim P}} \kappa(x, x') - 2 \mathbb{E}_{\substack{x \sim P \\ y \sim Q}} \kappa(x, y) + \mathbb{E}_{\substack{y \sim Q \\ y' \sim Q}} \kappa(y, y'), \quad (8)$$

which satisfies the metric properties, such as  $\text{MMD}(P, Q) = 0$  iff  $P = Q$  [24].

The MMD kernel used is defined as follows:

$$\kappa_{\mathcal{W}}(P, Q) = \exp\left(\frac{\mathcal{W}(P, Q)}{\sigma^2}\right) \quad (9)$$

in which  $\mathcal{W}$  is the Wasserstein distance and  $\sigma$  is a free parameter similar to a Radial Basis Function (RBF) kernel. This

function maintains the MMD assumptions, since it induces a unique RKHS [25], Proposition 2) and all statistical moments, which can be verified by the Taylor expansion of  $\kappa_{\mathcal{W}}$  [25].

The MMD for each graph metric was estimated using bootstrap sampling given the computational cost of MMD evaluation. This procedure consists of sampling 500 real graphs from the IGraphs dataset with replacement and assessing the MMD using these real graphs with other 500 synthetic graphs created by either baselines or our DGGI generator. This bootstrap evaluation was repeated 100 times, allowing for the establishment of a confidence interval associated with each MMD value.

### B. Training the DGGI Generator

Our dataset, IGraphs, was divided into three distinct parts: training, validation, and testing. All of the sample graphs from IGraphs were shuffled, and 70% of them were reserved for the training set, while the remaining graphs were divided equally for the validation and test sets. This partition led to a total of 63.229, 13.547, and 13.547 graphs for training, validation, and testing, respectively.

The DGGI generator learns the conditional distribution that models the link generation of the graphs in the training data, *i.e.*, given a previous graph state, the generator predicts a new link. Binary cross entropy [32] is used as the loss function since the prediction of links is mapped into a binary classification problem to determine if a link exists or not.

The machine used for training had an i7-9700 CPU and a Quadro RTX 6000 GPU. The training procedure consisted of 500 epochs using the Adaptive Moment Estimation (ADAM) optimizer [33] with an initial learning rate of 0.003 decaying by a factor of 0.3 when the training reaches 300 and 400 epochs. Backpropagation for each mini-batch composed of 40 graphs sampled from the training set was evaluated using uniform bootstrap sampling. The best model was determined based on the best MMD value obtained for the validation set, considering the node degree distribution.

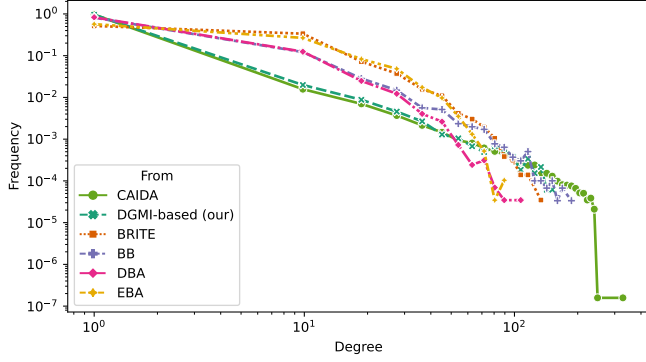
### C. Baselines

The adopted baseline generators were divided into two groups: generators based on the BA algorithm, BRITE, BB, EBA, and DBA, and those based on the structure-based models of SubNetG, S-BITE, IAG, and Orbis.

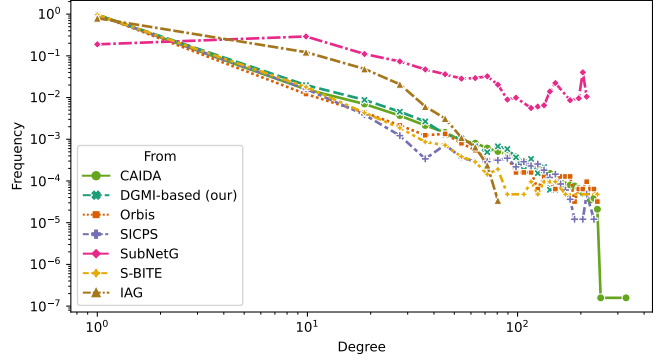
The BA-based models were configured using commonly used parameter values [6], [8], [26]. Each new node establishes two new links following preferential attachment. In BRITE, these links connect the new nodes with existing ones. EBA was configured to behave as BRITE 50% of the time, while 25% of the links were added to exiting nodes, and, for the other 25%, two known links were rewired. DBA uses two BA models at the same time, with 35% of the time, one link was added to any new node, instead of two links.

The size of the synthetic graphs generated by BA-based models was randomly determined. In order to improve the similarity between these graphs and IGraphs graphs, the size of a gamma function was fitted over the size distribution of CAIDA (Fig. 3).

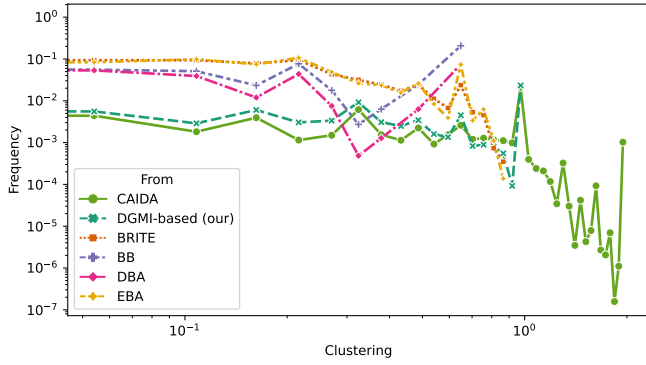




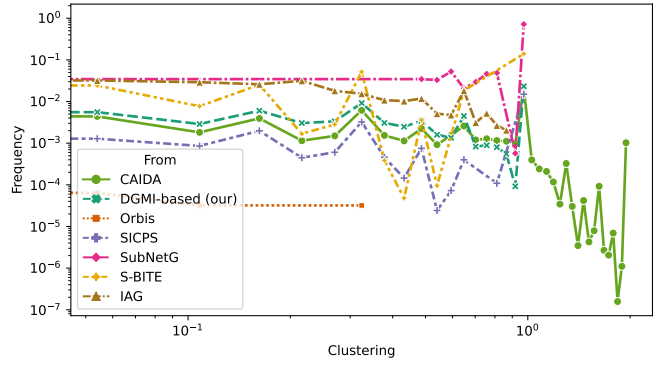
(a) BA-based baselines.



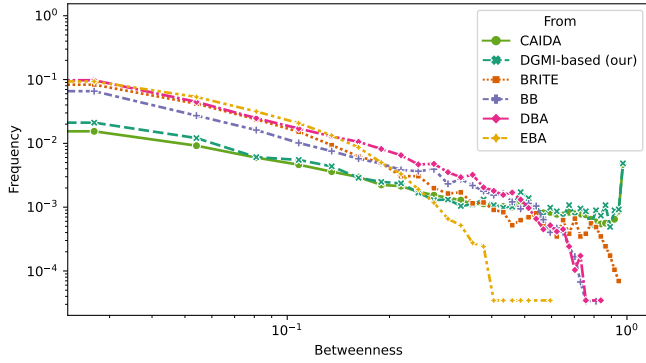
(b) Structure-based baselines.



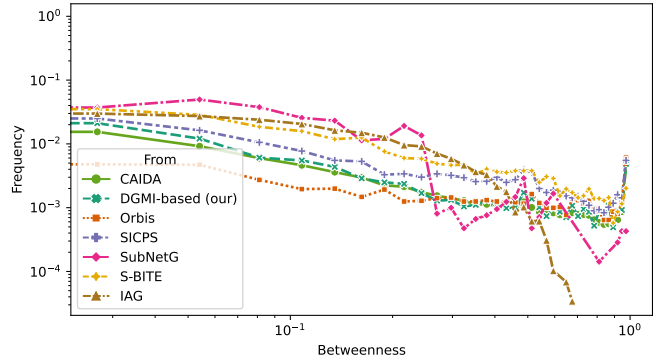
(c) BA-based baselines.



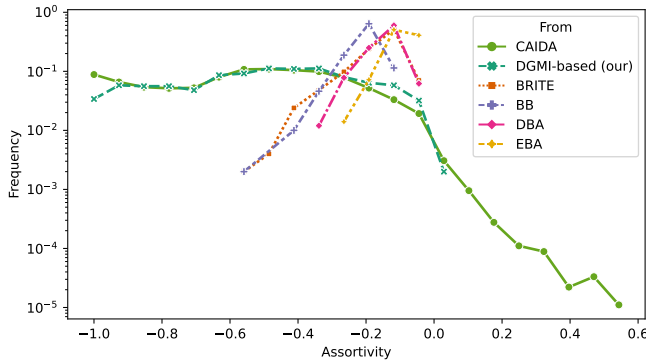
(d) Structure-based baselines.



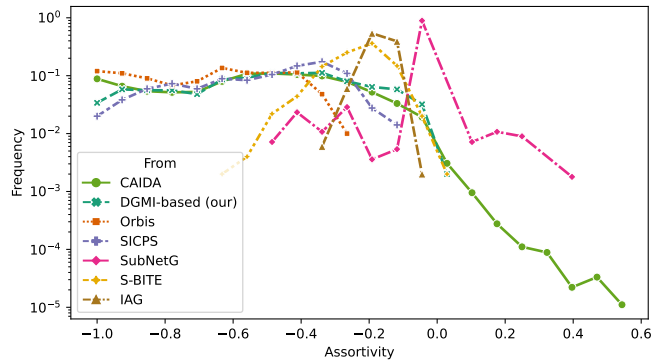
(e) BA-based baselines.



(f) Structure-based baselines.



(g) BA-based baselines.



(h) Structure-based baselines.

Fig. 6. The frequency distribution for the occurrence of each assessed graph metric. For the sake of comparison, all graphs present the distribution for CAIDA and for our model, DGMI, and the baselines are organized in two groups, BA and structure-based.

TABLE II  
ACHIEVED AVERAGE MMD FOR DIFFERENT GRAPH METRICS

Generator	MMD Assortativity	MMD Betweenness	MMD Clustering	MMD Node Degree
BB	$1.58e+00 \pm 4.03e-02$	$4.67e-02 \pm 2.25e-03$	$9.62e-01 \pm 2.64e-02$	$8.95e-01 \pm 1.26e-02$
BRITE	$1.70e+00 \pm 3.22e-02$	$5.68e-02 \pm 2.57e-03$	$4.54e-01 \pm 1.44e-02$	$5.62e-01 \pm 1.26e-02$
DBA	$1.75e+00 \pm 3.28e-02$	$7.99e-02 \pm 2.77e-03$	$4.16e-01 \pm 2.32e-02$	$1.06e+00 \pm 1.33e-02$
EBA	$1.85e+00 \pm 1.95e-02$	$1.04e-01 \pm 4.16e-03$	$8.54e-01 \pm 2.26e-02$	$6.86e-01 \pm 1.26e-02$
IAG	$1.69e+00 \pm 3.36e-02$	$7.87e-02 \pm 3.39e-03$	$3.45e-01 \pm 1.75e-02$	$8.51e-01 \pm 1.33e-02$
Orbis	$3.49e-01 \pm 5.63e-02$	$4.59e-03 \pm 7.33e-04$	$5.02e-02 \pm 7.29e-03$	$2.35e-02 \pm 3.04e-03$
S-BITE	$1.45e+00 \pm 5.17e-02$	$1.19e-01 \pm 8.64e-03$	$6.24e-01 \pm 2.49e-02$	$3.23e-01 \pm 1.69e-02$
SICPS	$8.70e-02 \pm 2.18e-02$	$4.17e-02 \pm 5.50e-03$	$2.76e-02 \pm 5.37e-03$	$6.27e-02 \pm 9.18e-03$
SubNetG	$1.68e+00 \pm 3.66e-02$	$1.03e-01 \pm 6.49e-03$	$1.54e+00 \pm 1.76e-02$	$5.95e-01 \pm 1.23e-02$
DGGI (our)	<b><math>7.56e-02 \pm 3.26e-02</math></b>	<b><math>1.31e-03 \pm 8.77e-04</math></b>	<b><math>2.80e-03 \pm 1.54e-03</math></b>	<b><math>6.82e-03 \pm 2.17e-03</math></b>

On the other hand, for structure-based models, the used configurations followed the parameters suggested in [12]–[14], [17]. For S-BITE and SubNetG, the parameters were determined using topologies provided by the IRL-based dataset [13], [14]. The joint distribution of node degrees required by Orbis was extracted from the AS topology of CAIDA (Section V). Moreover, IAG did not require any further configuration.

In contrast to BA-based models, S-BITE, SubNetG, and Orbis models were designed to generate graphs in the range of hundreds of thousands of nodes. Since graphs with hundreds of nodes are expected, the FRM algorithm was used to extract small subgraphs from the large synthetic graphs provided by those baselines (Section V).

#### D. Results and Discussion

We aim at assessing the similarity of the graphs synthesized by the DGGI generator in relation to those of the test set extracted from IGraphs (Section VI-B). The same comparison was performed for the baseline generators. The similarity is quantified using both first and higher moments of the following four graph metrics: node degree, clustering, betweenness, and assortativity.

Fig. 6 shows the distributions of all mentioned graph metrics. Based on these distributions, it can be inferred that the DGGI generator reproduces the test set distribution accurately for all assessed metrics. Figures 6a, 6c, 6e, and 6g indicate that those based on the BA method (*i.e.*, BRITE, BB, EBA, DBA) do not reproduce the test set distribution for all metrics.

For structure-based baselines, Figures 6b, 6d, 6f, and 6h show that neither IAG nor SubNetG succeed in reproducing the test set distributions. Orbis and SICPS can visually decrease the overall distance with respect to the test set distributions for the node degree, betweenness, and assortativity. However, the clustering distribution is not reproduced accurately by Orbis, and S-BITE does not reproduce the test set distribution for the clustering, betweenness, and assortativity metrics.

These results suggest that the DGGI generator overperforms all other generators considered, *i.e.*, this generator can synthesize graphs with the greatest similarity to the test set. However, the distributions in Fig. 6 only allow a visual comparison and give a limited notion of mean, variance, and other higher moments. Thus, the MMD was used to represent the differences with respect to the test set of these statistical moments in a concise form. Table II shows the MMD values for each generator assessed for the four graph metrics. The assessment based on these values shows that DGGI leads to the production of synthesized graphs that best represent the real-world intra-AS graphs found in the test set.

## VII. CONCLUSIONS

This paper introduced DGGI, a novel intra-AS graph generator. It also introduces a novel dataset (IGraphs) composed of real intra-AS graphs and a parameterized algorithm for subgraphs extraction (FRM), which ensures that subgraphs are within predefined limits for a number of nodes without losing the original characteristics of the graph formation process.

The percent differences between the values given by DGGI and those given by the baseline generators were computed. Experimental results demonstrate that the DGGI generator over performs all baseline generators. On average, DGGI improved the Maximum Mean Discrepancy ( $84.4 \pm 27.3\%$ ), ( $95.1 \pm 8.9\%$ ), ( $97.9 \pm 3.5\%$ ), and ( $94.7 \pm 9.5\%$ ), for assortativity, betweenness, clustering, and node degree, respectively. In the worst scenario, DGGI improved 13.1% the assortativity, and, in the best scenario, it reached 99.8% in clustering (Table III).

IGraphs is the first dataset that shows such a wide variety of real-world intra-AS graphs and offers novel possibilities for the analysis of solutions for the Internet. IGraphs provides the possibility of training data-driven models based on graphs using only real-world topologies and improving the generalization capacity of models due to the variety of graphs. IGraphs can also be used to diversify the simulation and emulation of solutions for the Internet.

TABLE III  
ACHIEVED AVERAGE IMPROVEMENTS USING DGGI

Baselines	Assortativity	Betweenness	Clustering	Node Degree
BB	95.22%	97.19%	99.71%	99.24%
BRITE	95.56%	97.68%	99.38%	98.79%
DBA	95.68%	98.35%	99.33%	99.35%
EBA	95.91%	98.74%	99.67%	99.01%
IAG	95.54%	98.33%	99.19%	99.2%
Orbis	78.31%	71.35%	94.43%	70.93%
S-BITE	94.78%	98.9%	99.55%	97.89%
SICPS	13.08%	96.85%	89.86%	89.11%
SubNetG	95.49%	98.72%	99.82%	98.85%

Future work encompasses the investigation of the use of DGGI for graph-based learning algorithms in network applications [3]–[5]. We also plan to develop a user interface for DGGI to help synthesize graphs for intra-AS networks.

#### ACKNOWLEDGMENTS

The authors would like to thank CAPES (grant #88882.329131/2019–01). Authors are also grateful to CNPq (grant #307560/2016-3), São Paulo Research Foundation – FAPESP (grants #2014/12236-1, #2015/24494-8, and #2016/50250-1, #2017/20945-0).

#### REFERENCES

- [1] C. Labovitz, A. Ahuja, R. Wattenhofer, and S. Venkataschary, “The impact of internet policy and topology on delayed routing convergence,” in *Proceedings IEEE INFOCOM 2001. Conference on Computer Communications. Twentieth Annual Joint Conference of the IEEE Computer and Communications Society (Cat. No. 01CH37213)*, IEEE, vol. 1, 2001, pp. 537–546.
- [2] M. H. Gunes and K. Sarac, “Importance of ip alias resolution in sampling internet topologies,” in *2007 IEEE Global Internet Symposium*, IEEE, 2007, pp. 19–24.
- [3] J. Suárez-Varela, P. Almasan, M. Ferriol-Galmés, et al., “Graph neural networks for communication networks: Context, use cases and opportunities,” *IEEE Network*, 2022.
- [4] F. Tang, B. Mao, Y. Kawamoto, and N. Kato, “Survey on machine learning for intelligent end-to-end communication toward 6g: From network access, routing to traffic control and streaming adaption,” *IEEE Communications Surveys & Tutorials*, vol. 23, no. 3, pp. 1578–1598, 2021.
- [5] W. Jiang, “Graph-based deep learning for communication networks: A survey,” *Computer Communications*, 2021.
- [6] S.-H. Yook, H. Jeong, and A.-L. Barabási, “Modeling the internet’s large-scale topology,” *Proceedings of the National Academy of Sciences*, vol. 99, no. 21, pp. 13 382–13 386, 2002.
- [7] A.-L. Barabási and R. Albert, “Emergence of scaling in random networks,” *science*, vol. 286, no. 5439, pp. 509–512, 1999.
- [8] A. Medina, A. Lakhina, I. Matta, and J. Byers, “Brite: An approach to universal topology generation,” in *MASCOTS 2001, Proceedings Ninth International Symposium on Modeling, Analysis and Simulation of Computer and Telecommunication Systems*, IEEE, 2001, pp. 346–353.
- [9] N. Moshiri, “The dual-barabási-albert model,” *arXiv preprint arXiv:1810.10538*, 2018.
- [10] G. Bianconi and A.-L. Barabási, “Competition and multiscaling in evolving networks,” *EPL (Europhysics Letters)*, vol. 54, no. 4, p. 436, 2001.
- [11] R. Albert and A.-L. Barabási, “Topology of evolving networks: Local events and universality,” *Physical review letters*, vol. 85, no. 24, p. 5234, 2000.
- [12] B. Jiao and W. Zhang, “Structural decomposition model for the evolution of as-level internet topologies,” *IEEE Access*, vol. 8, pp. 175 277–175 296, 2020.
- [13] K. Bakhshaliyev and M. H. Gunes, “Generation of 2-mode scale-free graphs for link-level internet topology modeling,” *Plos one*, vol. 15, no. 11, 2020.
- [14] G. Accongiagioco, E. Gregori, and L. Lenzini, “S-bite: A structure-based internet topology generator,” *Computer Networks*, vol. 77, pp. 73–89, 2015.
- [15] T. Lappas, K. Pelechrinis, M. Faloutsos, and S. V. Krishnamurthy, “A simple conceptual generator for the internet graph,” in *2010 17th IEEE Workshop on Local Metropolitan Area Networks (LANMAN)*, 2010, pp. 1–6.
- [16] A. Elmokashfi, A. Kvalbein, and C. Dovrolis, “On the scalability of bgp: The role of topology growth,” *IEEE Journal on Selected Areas in Communications*, vol. 28, no. 8, pp. 1250–1261, 2010.
- [17] P. Mahadevan, C. Hubble, D. Krioukov, B. Huffaker, and A. Vahdat, “Orbis: Rescaling degree correlations to generate annotated internet topologies,” in *Proceedings of the 2007 Conference on Applications, Technologies, Architectures, and Protocols for Computer Communications*, ser. SIGCOMM ’07, Association for Computing Machinery, 2007, pp. 325–336.
- [18] M. A. Canbaz, K. Bakhshaliyev, and M. H. Gunes, “Router-level topologies of autonomous systems,” in *International Workshop on Complex Networks*, Springer, 2018, pp. 243–257.

- [19] M. Latapy and C. Magnien, “Complex network measurements: Estimating the relevance of observed properties,” in *IEEE INFOCOM 2008-The 27th Conference on Computer Communications*, IEEE, 2008, pp. 1660–1668.
- [20] R. Albert, H. Jeong, and A.-L. Barabási, “Error and attack tolerance of complex networks,” *nature*, vol. 406, no. 6794, pp. 378–382, 2000.
- [21] M. H. Gunes, S. Bilir, K. Sarac, and T. Korkmaz, “A measurement study on overhead distribution of value-added internet services,” *Computer Networks*, vol. 51, no. 14, pp. 4153–4173, 2007.
- [22] N. Hidaka, S. Arakawa, and M. Murata, “A modeling method for isp topologies based on network-cost optimization,” in *Fourth International Conference on Autonomic and Autonomous Systems (ICAS’08)*, IEEE, 2008, pp. 169–174.
- [23] *The caida macroscopic internet topology data kit - 2020-08*. [Online]. Available: <https://www.caida.org/catalog/datasets/internet-topology-data-kit>.
- [24] A. Gretton, K. Borgwardt, M. Rasch, B. Schölkopf, and A. Smola, “A kernel method for the two-sample problem,” *Advances in neural information processing systems*, vol. 19, 2006.
- [25] J. You, R. Ying, X. Ren, W. Hamilton, and J. Leskovec, “Graphrnn: Generating realistic graphs with deep autoregressive models,” in *International conference on machine learning*, PMLR, 2018, pp. 5708–5717.
- [26] A. Vázquez, R. Pastor-Satorras, and A. Vespignani, “Large-scale topological and dynamical properties of the internet,” *Physical Review E*, vol. 65, no. 6, p. 066 130, 2002.
- [27] L. d. F. Costa, F. A. Rodrigues, G. Travieso, and P. R. Villas Boas, “Characterization of complex networks: A survey of measurements,” *Advances in physics*, vol. 56, no. 1, pp. 167–242, 2007.
- [28] V. D. Blondel, J.-L. Guillaume, R. Lambiotte, and E. Lefebvre, “Fast unfolding of communities in large networks,” *Journal of statistical mechanics: theory and experiment*, vol. 2008, no. 10, P10008, 2008.
- [29] K. Cho, B. van Merriënboer, D. Bahdanau, and Y. Bengio, “On the properties of neural machine translation: Encoder–decoder approaches,” in *8th Workshop on Syntax, Semantics and Structure in Statistical Translation, SSST 2014*, Association for Computational Linguistics (ACL), 2014, pp. 103–111.
- [30] B. Zhang, R. Liu, D. Massey, and L. Zhang, “Collecting the internet as-level topology,” *ACM SIGCOMM Computer Communication Review*, vol. 35, no. 1, pp. 53–61, 2005.
- [31] S. Knight, H. X. Nguyen, N. Falkner, R. Bowden, and M. Roughan, “The internet topology zoo,” *IEEE Journal on Selected Areas in Communications*, vol. 29, no. 9, pp. 1765–1775, 2011.
- [32] F. Topsøe, “Bounds for entropy and divergence for distributions over a two-element set,” *J. Ineq. Pure & Appl. Math*, vol. 2, no. 2, p. 300, 2001.
- [33] D. P. K. JLB, “Adam: A method for stochastic optimization,” in *3rd international conference for learning representations, San Diego*, 2015.